Available online at http://scik.org
Commun. Math. Biol. Neurosci. 2024, 2024:15
https://doi.org/10.28919/cmbn/8381
ISSN: 2052-2541

GLOBAL STABILITY ANALYSIS AND OPTIMAL CONTROL PROBLEM ARISE FROM TUBERCULOSIS TRANSMISSION MODEL WITH MONITORED TREATMENT

PUTRI ZAHRA KAMALIA*, TIARA AYUMI, ATHAYA YUMNA FATHIYAH, DIPO ALDILA

Department of Mathematics, Faculty of Mathematics and Natural Sciences, Universitas Indonesia, Depok 16424, Indonesia

Abstract. In this paper, we discussed a Tuberculosis model by incorporating monitored treatment intervention and applying optimal control theory to analyze the optimal intervention for TB. Optimal control strategy aims to minimize both the disease burden and the intervention cost. The optimal control problem is derived analytically using the Pontryagin Maximum Principle. Analysis of the model shows that disease-free equilibrium is globally asymptotically stable if the controlled reproduction number is smaller than one and unstable if it is larger than one. Our numerical experiments show that implementation of monitored treatment should be given in the early spread of TB to avoid high cost of intervention. Furthermore, a better quality of treatment will give a lower cost for TB prevention.

Keywords: tuberculosis; monitored treatment; optimal control; reproduction number.

2010 AMS Subject Classification: 00A69, 37N25, 93D20.

1. INTRODUCTION

Tuberculosis (TB) is an infectious disease caused by *Mycobacterium tuberculosis*. It can attack the human organs including the lungs, kidney, spine, and brain. This infection is mainly

*Corresponding author
E-mail address: putri.zahra@sci.ui.ac.id
Received December 10, 2023

transmitted through the air when individuals with active TB cough, sneeze, speak, or sing. People who breathe air that has been contaminated by the bacteria will be infected with TB [10].

TB holds the thirteenth position in deadliest diseases and the second leading infectious killer after COVID-19 (above HIV and AIDS) in the world. Globally, in 2021, 10.6 million people are infected by TB which causes an average death rate of 1.4 million people with HIV-negative and 187,000 people co-infected with HIV. In 2021, the top three countries of TB patients are India, Indonesia, and Filipina [23].

If someone is infected by TB bacteria, the bacteria may not directly active and without making you sick. In these people, they do not show any symptoms and can not transmit TB to other individuals. It is called latent TB. If they have weak immune system and not receiving effective treatment, latent TB can develop into active TB. The symptoms of active TB are cough with blood for three weeks or more, weight loss, easy fatigue, fever, and night sweats [2].

One of the factors causing the high number of TB cases in the world is treatment failure due to non-compliance of TB patients in completing the treatment given and the lack of knowledge of TB patients. If they do not get treatment with the good procedure, it inhibits the healing process and also increases the potential for drug resistence [10]. In 1993, WHO launched the DOT (Directly Observed Treatment) program as TB disease treatment. DOT is face-to-face or online monitoring of TB patients while taking antituberculosis drugs. This strategy ensures that the drug consumption is carried out with the right combination and dose. Patients will be monitored daily by health workers or individuals who are trained when taking drugs. DOT strategy can reduce the rate of spread of TB with a more effective cost [22].

Mathematical modeling has been studied by many researchers to understand the spread of many diseases [3, 4, 5, 6, 7, 8, 9], including TB. Research by authos in [14] analyzed the spread of tuberculosis with recovery time delay. Wangari and Stone [21] analyzed the effect of TB recurrence through the SEIR mathematical model using a linear infection function. A simple SEIR model to discuss the local and global stability of TB transmisison model discussed by authors in [13]. Authors in [11] developed their TB model by considering the impact of media

awareness on the population. Multiple re-infection on TB discussed by authors in [12]. Recently, authors in [1] proposed a mathematical model to assess the potention of new TB vaccine in controlling TB transmission. To control the spread of TB disease, several mathematical models implement it as an optimal control problem such as research conducted by D.Aldila et al. [29] that discussed about optimal control problem from tuberculosis and MDR-TB model.

Based on above description and the urgency of monitored treatment, it is necessary to understand the impact of monitored treatment for TB controlling scenario for long run intervention. Hence, we construct an optimal control problem model for TB transmission in this article considering monitored treatment as a single intervention for TB control. We modify the model by authors in [13] by adding a proportion of treated individual into the model as a time-dependent parameter. Mathematical analysis such as local and global stability analysis for the autonomous model conducted to see the possible final condition of the population. Characterization of the optimal control problem using Pontryagin Maximum Principle used, and solved using the forward-backward sweep algorithm.

The layout of this article is as follows. In the next section, model construction and it preliminary analysis conducted. In Section 3, mathematical analysis of the model related to equilibrium points and the basic reproduction number is given. We conduct optimal control problems using monitored treatment as control variable in Section 4. Finally, some conclusions are given in Section 5.

2. THE MODEL

2.1. Model Construction. The population is assumed to be closed and constant over time. In other words, influxes/outfluxes coming from migrations or emigrations are considered inessential. Also, the recruitment rate and natural death rates are assumed to be equal. We divided the human population into four compartments, which are the susceptible (S), the exposed or latent TB (E), the infected or active TB (I), and recovered (R).

- *Susceptible*. The susceptible compartment contains healthy individuals who have never been infected by TB before, including newborns.

- *Exposed.* This exposed compartment classifies the individuals who have already been infected by TB but are not yet infective. The individuals in this compartment do not feel sick and the disease cannot be detected unless they get a TB skin test or TB blood test. The TB bacteria's status in this compartment is dormant residing in human lungs, constrained by host immune responses. It is known as latent TB infection/LTBI.
- *Infected.* Latent TB individuals can progress to active TB depending on their immune system. Active TB individuals may get sick and can spread the bacteria to susceptible individuals. Active TB individuals develop symptoms such as coughing for more than three weeks (often with blood), fever, chest pain, and loss of appetite.
- *Recovered.* This compartment contains individuals who have recovered from TB disease, both with monitored care and unmonitored care. We assume that recovered individual have permanent immunity.

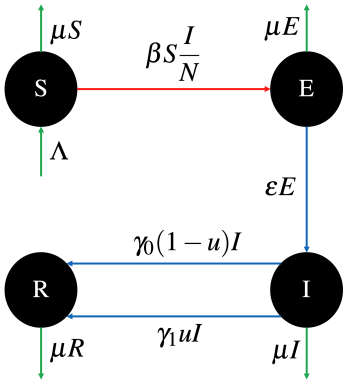

FIGURE 1. Transmission Diagram of Tuberculosis Spread

TABLE 1. Description of Parameters

Parameter	**Description**	**Value**	**Ref**
μ_1	Recruitment rate	0.012	[13]
μ_2	Natural death rate	0.012	[13]
β	Succesful infection rate	[0.0868, 0.2568]	[13]
ε	Transition rate from TB-passive to TB-active	0.148	[13]
γ_1	Recovery rate based on monitored treatment	0.104	[13]
γ_0	Recovery rate based on unmonitored treatment	0.416	[13]
u	Proportion of human who get monitored treatment	[0,1]	Assumed
$1-u$	Proportion of human who do not get monitored treatment	[0,1]	Assumed

We use transmission diagram in Figure 1 for model construction. Description of the parameters that are used could be seen in Table 1. Susceptible increase due to a new born with a constant rate Λ. We assume that only individuals in I compartment can spread TB to the susceptible individuals with a constant rate β. Assuming a ratio dependent contact rate for the infection term, we have the rate of new infection is given by $\frac{\beta SI}{N}$. After period of incubation, denoted by ε^{-1}, exposed individual in E progress to I individuals. We assume that only proportion of u of I who get a monitored treatment by the hospital. Infected individuals who get monitored treatment can recovered with a rate of γ_1, while who do not will recovered with a rate of γ_0. Note that $\gamma_0 < \gamma_1$. Each compartment can decreases due to natural death rate μ.

Based on the assumptions and transmission diagram in Figure 1, the model for TB transmission with the impact of monitored treatment is given by:

$$\begin{aligned}
\frac{dS}{dt} &= \Lambda - \mu S - \beta S\frac{I}{N},\\
\frac{dE}{dt} &= \beta S\frac{I}{N} - \mu E - \varepsilon E,\\
\frac{dI}{dt} &= \varepsilon E - \mu I - \gamma_1 uI - \gamma_0(1-u)I,\\
\frac{dR}{dt} &= \gamma_1 uI + \gamma_0(1-u)I - \mu R,
\end{aligned} \tag{1}$$

where $N = S+E+I+R$ is the total human population. We assumed that the human population is constant, which gives us $\Lambda = \mu N$. With this assumption, we scale the human sub-populations. Let $s = \frac{S}{N}$, $e = \frac{E}{N}$, $i = \frac{I}{N}$, and $r = \frac{R}{N}$ represents the fraction of each compartment in the population. Hence, the non-dimensional form of model variables of system (1) is given by:

$$\begin{aligned}
\frac{ds}{dt} &= \mu - \mu s - \beta si = 0,\\
\frac{de}{dt} &= \beta si - \mu e - \varepsilon e = 0,\\
\frac{di}{dt} &= \varepsilon e - \mu i - \gamma_1 ui - \gamma_0(1-u)i = 0,\\
\frac{dr}{dt} &= \gamma_1 ui + \gamma_0(1-u)i - \mu r = 0,
\end{aligned} \tag{2}$$

where

$$s+e+i+r = 1,$$

and with the initial condition

$$s(0) = s_0 > 0, e(0) = e_0 > 0, i(0) = i_0 > 0, \text{ and } r(0) = r_0 > 0.$$

2.2. Preliminary analysis. Since the non-dimensional model in equation (2) presents the human population, then the solutions must be positive and bounded in a feasible region. In this section, we will verify that all the solutions of the model will always be positive and bounded for all $t > 0$. To assure these, we have the following theorem

Theorem 1. *Model* (2) *with the initial condition* $s(0) = s_0 > 0, e(0) = e_0 \geq 0, i(0) = i_0 \geq 0, r(0) = r_0 \geq 0$*, always has positive solutions for all* $t > 0$*.*

Proof. We use an integrating factor to solve this theorem. Under the given initial conditions, from the first equation of the TB model (2) we have

$$\frac{ds}{dt} = \mu - \mu s - \beta si.$$

Equation (3) can be written as

$$\frac{ds}{dt} + A(t)s = B(t).$$

where

$$A(t) = \mu + \beta i,$$

$$B(t) = \mu.$$

Define integrating factor $C(t) = e^{\int_0^t A(x)dx}$. Multiply equation (3) with the integrating factor. Hence, we have

$$e^{\int_0^t A(x)dx}\frac{ds}{dt} + e^{\int_0^t A(x)dx}A(t)s = e^{\int_0^t A(x)dx}B(t).$$

The equation (3) can be expressed as follows

$$\frac{d}{dt}\left(s(t)e^{\int_0^t A(x)dx}\right) = e^{\int_0^t A(x)dx}B(t),$$

$$d\left(s(t)e^{\int_0^t A(x)dx}\right) = e^{\int_0^t A(x)dx}B(t)dt.$$

By integrating both sides of the equation (3) in interval $[0,t]$, we obtain

$$s(t)e^{\int_0^t A(x)dx} - s(0) = \int_0^t e^{\int_0^x A(p)dp}B(x)dx,$$

$$s(t)e^{\int_0^t A(x)dx} = \int_0^t e^{\int_0^x A(p)dp} B(x)dx + s(0),$$

therefore

$$s(t) = e^{-\int_0^t A(x)dx}\left(\int_0^t e^{\int_0^x A(p)dp} B(x)dx + s(0)\right) > 0.$$

Hence, it can be shown that $s(t) > 0$ for all $t > 0$. In a similar way, $e(t), i(t), r(t)$ also can be shown positive under the given initial condition $s(0) = s_0 > 0, e(0) = e_0 \geq 0, i(0) = i_0 \geq 0, r(0) = r_0 \geq 0$. Thus, the solutions $s(t), e(t), i(t), r(t)$ of the model (2) are positive for all $t > 0$. □

Since the total population is assumed always be constant and all solutions of the model (2) are proven always positive, then we have that each compartment $s(t), e(t), i(t), r(t)$ is bounded at $[0, 1]$. Furthermore, the TB model has the positively invariant region as follows.

$$\Omega = \left\{s, e, i, r \in \mathbb{R}^4_+ : 0 < s \leq 1, 0 \leq e < 1, 0 \leq i < 1, 0 \leq r < 1, s + e + i + r = 1\right\}. \tag{3}$$

Corollary 1. *The region* $\Omega \in \mathbb{R}^4_+$ *is positively invariant for the model* (2) *with the initial condition* $\in \mathbb{R}^4_{\geq 0}$.

Therefore, we have that Ω is positively invariant and attract all the solutions in $\mathbb{R}^4_{\geq 0}$. Hence, model (2) is considered to be well-posed mathematically and epidemiologically.

3. Model Analysis

Since we have $s + e + i + r = 1$, then it is worth to analyze system (2) by only analyzing the first three equation, i.e:

$$\begin{aligned} \frac{ds}{dt} &= \mu - \mu s - \beta si = 0, \\ \frac{de}{dt} &= \beta si - \mu e - \varepsilon e = 0, \\ \frac{di}{dt} &= \varepsilon e - \mu i - \gamma_1 ui - \gamma_0(1-u)i = 0, \end{aligned} \tag{4}$$

where r can be determined as $r = 1 - s - e - i$. To determine the equilibrium point of the model (4), we need to solve the left hand side of system (4) equals to 0, which $\frac{ds}{dt} = \frac{de}{dt} = \frac{di}{dt} = 0$.

3.1. Disease-free equilibrium point and formulation $\mathscr{R}_0$. At the disease-free equilibrium point, it means that there are no humans infected by *Mycobacterium tuberculosis* when $e = 0, i = 0$ so there is no TB disease in the population. Therefore, the disease-free equilibrium point is given by

$$DFE = (s^*, e^*, i^*) = (1, 0, 0). \tag{5}$$

Theorem 2. *The Disease-free equilibrium point* (s^*, e^*, i^*) *in the model* (4) *will always be exists in the population without any condition.*

Using the next-generation matrix method [15], we determine the expression of basic reproduction number. It's given by

$$\mathscr{R}_0 = \frac{\varepsilon\beta}{(\mu+\varepsilon)(\mu+\gamma_1 u+\gamma_0(1-u))}. \tag{6}$$

Basic reproduction number ($\mathscr{R}_0$) is the expected number of secondary infection cases caused by a single infected individual in a susceptible population. for further examples on the calculation of $\mathscr{R}_0$ with this next-generation method can be seen in [16, 17, 18, 19, 20].

3.2. Endemic equilibrium point. Endemic-equilibrium point indicates that the infection will not be eradicated from the population. It will be determined when $e \neq 0$ and $i \neq 0$. Therefore, the endemic equilibrium point is given in the expression of $\mathscr{R}_0$ as follows

$$EE = (s^\dagger, e^\dagger, i^\dagger) = \left(\frac{1}{\mathscr{R}_0}, \frac{\mu(\mathscr{R}_0-1)}{\mathscr{R}_0(\mu+\varepsilon)}, \frac{\mu(\mathscr{R}_0-1)}{\beta}\right). \tag{7}$$

From the expression of EE in (7), we have the following theorem.

Theorem 3. *Endemic-equilibrium point* $(s^\dagger, e^\dagger, i^\dagger)$ *of model* (4) *exists if condition* $\mathscr{R}_0 > 1$ *holds.*

3.3. Stability of Disease Free Equilibrium.

3.3.1. *Local Stability Analysis of DFE.*

Theorem 4. *The DFE of TB model in* (4) *is locally asymptotically stable if* $\mathscr{R}_0 < 1$ *and unstable if* $\mathscr{R}_0 > 1$.

Proof. We use standard linearization to prove the theorem. Linearization around the disease-free equilibrium is given by

$$J|_{DFE} = \begin{bmatrix} -\mu & 0 & -\beta \\ 0 & -\mu-\varepsilon & \beta \\ 0 & \varepsilon & -\mu-\gamma_1 u-\gamma_0(1-u) \end{bmatrix}. \tag{8}$$

Next, calculate $|\lambda I - J|_{DFE}) = 0$ to get the characteristic equation of the matrix (8) as follows

$$(\lambda+\mu)(\lambda^2+(2\mu+\gamma_1 u+\gamma_0(1-u)+\varepsilon)\lambda+(\mu+\varepsilon)(\mu+\gamma_1 u+\gamma_0(1-u))-\varepsilon\beta = 0.$$

It can be seen from the equation (9), there is an eigenvalue that obviously negative which is $\lambda_1 = -\mu$, while the other two eigenvalues can be determined by Routh-Hurwitz criteria. Let

$$\lambda^2 + a_1\lambda + a_0 = 0, \tag{9}$$

where $a_1 = 2\mu+\gamma_1 u+\gamma_0(1-u)+\varepsilon$, and $a_0 = (\mu+\varepsilon)(\mu+\gamma_1 u+\gamma_0(1-u))-\varepsilon\beta$. The DFE is asymptotically stable if all the real parts of its eigenvalues are negative. By using Routh-Hurwitz criteria, the polynomial (9) has negative real parts if $a_0, a_1 > 0$. All of our parameters are positive, so that $a_1 > 0$. To prove that $a_0 > 0$, it must be

$$\frac{\varepsilon\beta}{(\mu+\varepsilon)(\mu+\gamma_1 u+\gamma_0(1-u))} < 1 \iff \mathscr{R}_0 < 1.$$

Hence, the DFE of model (4) is locally asymptotically stable if $\mathscr{R}_0 < 1$. □

3.3.2. *Global Stability Analysis of DFE.*

Theorem 5. *The DFE of TB model in* (4) *is globally asymptotically stable if* $\mathscr{R}_0 < 1$ *and unstable if* $\mathscr{R}_0 > 1$.

Proof. Now we prove that the disease-free equilibrium point is globally asymptotically stable. We use the following Lyapunov function for the model (4):

$$V(e,i) = \phi_1 e + \phi_2 i. \tag{10}$$

where e and i are the compartments of the model (4) and the coefficient $\phi_1, \phi_2 > 0$ is to be determined. Since the solutions e and i are positive, obviously $V(e,i)$ is always positive and

$V(e^*,i^*)=0$ when $e^*=i^*=0$. Furthermore, $V(e,i)$ is also radially unbounded. Differentiating the function with respect to t along the solutions of the model (4), we have

$$V'(e,i)=\phi_1 e'+\phi_2 i'.$$

Replacing e' and i' with their the model equations in (4), we have

$$V'(e,i)=\phi_1(\beta s^* i^*-\mu e^*-\varepsilon e^*)+\phi_2(\varepsilon e^*-\mu i^*-\gamma_1 u i^*-\gamma_0(1-u)i^*).$$

By choosing $\phi_1=\frac{\varepsilon}{\mu+\varepsilon}$ and $\phi_2=1$, we got

$$\begin{aligned}
V'(e,i) &= \frac{\varepsilon}{\mu+\varepsilon}(\beta s^* i^*-\mu e^*-\varepsilon e^*)+(\varepsilon e^*-\mu i^*-\gamma_1 u i^*-\gamma_0(1-u)i^*),\\
&= \frac{\varepsilon}{\mu+\varepsilon}(\beta s^* i^*-(\mu+\varepsilon)e^*)+(\varepsilon e^*-(\mu+\gamma_1 u+\gamma_0(1-u))i^*),\\
&= \frac{\varepsilon\beta s^* i^*}{\mu+\varepsilon}-\varepsilon e^*+\varepsilon e^*-(\mu+\gamma_1 u+\gamma_0(1-u))i^*,\\
&= \frac{\varepsilon\beta s^* i^*}{\mu+\varepsilon}-(\mu+\gamma_1 u+\gamma_0(1-u))i^*,\\
&= i^*(\mu+\gamma_1 u+\gamma_0(1-u))\left(\frac{\varepsilon\beta}{(\mu+\varepsilon)(\mu+\gamma_1 u+\gamma_0(1-u))}-1\right),\\
&= i^*(\mu+\gamma_1 u+\gamma_0(1-u))(\mathscr{R}_0-1).
\end{aligned}$$

Since all parameters are positive, we have $V'(e,i)<0$ if $\mathscr{R}_0<1$ and $(e,i)\neq(e^*,i^*)$. Since $V(e,i)$ is a function that is positive definite, radially unbounded, and $V'(e,i)<0$, we conclude that the DFE of model in (4) is globally asymptotically stable when $\mathscr{R}_0<1$. □

3.4. Stability of Endemic Equilibrium.

3.4.1. *Local Stability Analysis of EE.*

Theorem 6. *The EE of the TB model* (4) *is locally asymptotically stable if* $\mathscr{R}_0>1$.

Proof. From the linearization, we obtain the following characteristic equation for EE

$$a_0\lambda^3+a_1\lambda^2+a_2\lambda+a_3=0, \tag{11}$$

where

$$
\begin{aligned}
a_0 &= 1,\\
a_1 &= 3\mu+\gamma_1 u+\gamma_0(1-u)+\varepsilon+\beta i^{\dagger},\\
a_2 &= (\mu+\varepsilon)(\mu+\gamma_1 u+\gamma_0(1-u))-\varepsilon\beta s^{\dagger}+(2\mu+\gamma_1 u+\gamma_0(1-u)+\varepsilon)(\mu+\beta i^{\dagger}),\\
a_3 &= (\mu+\beta i^{\dagger})((\mu+\varepsilon)(\mu+\gamma_1 u+\gamma_0(1-u))-\varepsilon\beta s^{\dagger})+\varepsilon\beta^2 s^{\dagger} i^{\dagger}.
\end{aligned}
\tag{12}
$$

By using the Routh-Hurwitz criteria, we can analyze the local stability of EE. The cubic polynomial in equation (11) has the negative real parts if all the coefficients in equation (12) are positive and $det(H_i) > 0, \forall_i = 1,2,3$. So, we define three matrices H as follows

$$
H_1 = \begin{bmatrix} a_1 \end{bmatrix},
$$

$$
H_2 = \begin{bmatrix} a_1 & 1 \\ 0 & a_2 \end{bmatrix},
$$

$$
H_3 = \begin{bmatrix} a_1 & 1 & 0 \\ a_3 & a_2 & a_1 \\ 0 & 0 & a_3 \end{bmatrix},
$$

where a_1, a_2, a_3 are coefficient that written in equation (12). Then, we know that $det(H_1) = a_1 > 0$ and $det(H_2) = a_1 a_2 > 0$ because $a_1, a_2 > 0$. Meanwhile, $det(H_3)$ is positive if $\mathscr{R}_0 > 1$. Hence, the EE of model(4) is locally asymptotically stable if $\mathscr{R}_0 > 1$. □

3.4.2. *Global Stability Analysis of EE.*

Theorem 7. *The EE of the TB model* (4) *is globally asymptotically stable if* $\mathscr{R}_0 > 1$.

Proof. Let

$$
V(s,e,i) = \kappa_1\left(s - s^{\dagger} - s^{\dagger}\ln\frac{s}{s^{\dagger}}\right) + \kappa_2\left(e - e^{\dagger} - e^{\dagger}\ln\frac{e}{e^{\dagger}}\right) + \kappa_3\left(i - i^{\dagger} - i^{\dagger}\ln\frac{i}{i^{\dagger}}\right),
\tag{13}
$$

be the Lyapunov function to proof the global stability of EE where the coefficient $\kappa_1 > 0, \kappa_2 > 0, \kappa_3 > 0$ will be determined later. Notice that $V(s,e,i) = 0$ when $(s,e,i) = (s^{\dagger}, e^{\dagger}, i^{\dagger})$. To establish $V(s,e,i) > 0$, notice that from equation (13)

$$
\kappa_1\left(s - s^{\dagger} - s^{\dagger}\ln\frac{s}{s^{\dagger}}\right) = \kappa_1 s^{\dagger}\left(\frac{s}{s^{\dagger}} - 1 - \ln\frac{s}{s^{\dagger}}\right),
$$

where $\kappa_1 s^\dagger$ always positive. If we set $x = \frac{s}{s^\dagger}$ such that

$$\kappa_1 s^\dagger \left(\frac{s}{s^\dagger} - 1 - \ln \frac{s}{s^\dagger}\right) = \kappa_1 s^\dagger (x - 1 - \ln x).$$

Set $g(x) = x - 1 - \ln x$. Note that $g(x)$ achieves a global minimum at $x = 1$ and $g(1) = 0$. Hence $g(x) > 0$ for all $x > 0$ and $\neq 1$. So the first term of $V(s,e,i)$ is positive. In a similar way, the remaining two terms are also positive. $V(s,e,i)$ is also radially unbounded. Then, we take the derivative of $V(s,e,i)$ with respect to t and replace s', e', and i' with the model equations in (4), we have

$$\begin{aligned} V'(s,e,i) =& \kappa_1 \left(1 - \frac{s^\dagger}{s}\right) s' + \kappa_2 \left(1 - \frac{e^\dagger}{e}\right) e' + \kappa_3 \left(1 - \frac{i^\dagger}{i}\right) i', \\ =& \kappa_1 \left(1 - \frac{s^\dagger}{s}\right) (\mu - \mu s - \beta s i) + \kappa_2 \left(1 - \frac{e^\dagger}{e}\right) (\beta s i - (\mu + \varepsilon) e) \\ &+ \kappa_3 \left(1 - \frac{i^\dagger}{i}\right) (\varepsilon e - (\mu + \gamma_1 u + \gamma_0 (1-u)) i). \end{aligned} \tag{14}$$

Replacing μ with $\mu = \frac{\beta s^\dagger i^\dagger}{(1 - s^\dagger)}$ or can be rewritten with $\mu = \mu s^\dagger + \beta s^\dagger i^\dagger$. Then, $\mu s^\dagger - \mu s$ can be combined with the first term in the product to yield a negative term.

$$\begin{aligned} V'(s,e,i) =& \kappa_1 \left(1 - \frac{s^\dagger}{s}\right) (-\mu (s - s^\dagger) + \beta s^\dagger i^\dagger - \beta s i) + \kappa_2 \left(1 - \frac{e^\dagger}{e}\right) (\beta s i - (\mu + \varepsilon) e) \\ &+ \kappa_3 \left(1 - \frac{i^\dagger}{i}\right) (\varepsilon e - (\mu + \gamma_1 u + \gamma_0 (1-u)) i). \end{aligned} \tag{15}$$

We multiply out all other products, then

$$\begin{aligned} V'(s,e,i) =& -\mu \kappa_1 \frac{(s - s^\dagger)^2}{s} + \kappa_1 \beta s^\dagger i^\dagger - \kappa_1 \beta s i - \kappa_1 \beta \frac{{s^\dagger}^2 i^\dagger}{s} + \kappa_1 \beta s^\dagger i + \kappa_2 \beta s i \\ &- \kappa_2 (\mu + \varepsilon) e - \kappa_2 \beta \frac{e^\dagger s i}{e} + \kappa_2 (\mu + \varepsilon) e^\dagger + \kappa_3 \varepsilon e - \kappa_3 (\mu + \gamma_1 u + \gamma_0 (1-u)) i \\ &- \kappa_3 \varepsilon \frac{i^\dagger e}{i} + \kappa_3 (\mu + \gamma_1 u + \gamma_0 (1-u)) i^\dagger. \end{aligned} \tag{16}$$

If $\kappa_1 = \kappa_2$, then $\kappa_1 \beta s i$ in equation (16) can be cancelled with $\kappa_2 \beta s i$. Also, where we have fractions, we multiply and divide by the equilibrium value such that

$$
\begin{aligned}
V'(s,e,i) = &-\mu\kappa_1\frac{(s-s^\dagger)^2}{s}+\kappa_1\beta s^\dagger i^\dagger-\kappa_1\beta\frac{s^{\dagger 2}i^\dagger}{s}+\kappa_1\beta s^\dagger i-\kappa_2(\mu+\varepsilon)e\\
&-\kappa_2\beta s^\dagger i^\dagger\frac{e^\dagger si}{es^\dagger i^\dagger}+\kappa_2(\mu+\varepsilon)e^\dagger+\kappa_3\varepsilon e-\kappa_3(\mu+\gamma_1 u+\gamma_0(1-u))i\\
&-\kappa_3\varepsilon e^\dagger\frac{i^\dagger e}{ie^\dagger}+\kappa_3(\mu+\gamma_1 u+\gamma_0(1-u))i^\dagger.
\end{aligned}
\tag{17}
$$

We want to combine all constant terms with all fractional terms because all constant terms are positive and all fractional terms are negative. Notice that since $\kappa_1=\kappa_2$ we have $\beta s^\dagger i^\dagger = (\mu+\varepsilon)e^\dagger$ from the corresponding equilibrium equation of model (4). We need to choose κ_3 such that

$$\kappa_3(\mu+\gamma_1 u+\gamma_0(1-u))i^\dagger=\kappa_2(\mu+\varepsilon)e^\dagger,$$

$$\kappa_3(\mu+\gamma_1 u+\gamma_0(1-u))\frac{\varepsilon e^\dagger}{(\mu+\gamma_1 u+\gamma_0(1-u))}=\kappa_2(\mu+\varepsilon)e^\dagger.$$

Hence,

$$\kappa_3=\kappa_2\frac{(\mu+\varepsilon)}{\varepsilon}.$$

Then, we pull out $\kappa_1\beta s^\dagger i^\dagger$ from all terms. We have

$$
\begin{aligned}
V'(s,e,i) = &-\mu\kappa_1\frac{(s-s^\dagger)^2}{s}+\kappa_1\beta s^\dagger i^\dagger\left[3-\frac{s^\dagger}{s}-\frac{e^\dagger si}{es^\dagger i^\dagger}-\frac{i^\dagger e}{ie^\dagger}\right]\\
&+(\kappa_1\beta s^\dagger-\kappa_3(\mu+\gamma_1 u+\gamma_0(1-u)))i+(\kappa_3\varepsilon-\kappa_2(\mu+\varepsilon))e
\end{aligned}
\tag{18}
$$

Because $\kappa_3=\kappa_2\frac{(\mu+\varepsilon)}{\varepsilon}$, so the last two terms in the equation (18) are zero. We know that $\mathscr{R}_0=\frac{\varepsilon\beta}{(\mu+\varepsilon)(\mu+\gamma_1 u+\gamma_0(1-u))}$, so we can replace β in the second term with $\beta=\frac{(\mu+\varepsilon)(\mu+\gamma_1 u+\gamma_0(1-u))\mathscr{R}_0}{\varepsilon}$. Then

$$V'(s,e,i)=-\mu\kappa_1\frac{(s-s^\dagger)^2}{s}+\kappa_1\frac{(\mu+\varepsilon)(\mu+\gamma_1 u+\gamma_0(1-u))\mathscr{R}_0}{\varepsilon}s^\dagger i^\dagger\left[3-\frac{s^\dagger}{s}-\frac{e^\dagger si}{es^\dagger i^\dagger}-\frac{i^\dagger e}{ie^\dagger}\right]$$

By choose $\kappa_1=\kappa_2=1$, and $\kappa_3=\frac{\mu+\varepsilon}{\varepsilon}$, we have

$$V'(s,e,i)=-\mu\frac{(s-s^\dagger)^2}{s}+\frac{(\mu+\varepsilon)(\mu+\gamma_1 u+\gamma_0(1-u))\mathscr{R}_0}{\varepsilon}s^\dagger i^\dagger\left[3-\frac{s^\dagger}{s}-\frac{e^\dagger si}{es^\dagger i^\dagger}-\frac{i^\dagger e}{ie^\dagger}\right]\tag{19}$$

The first term in equation (19) must be negative unless $s=s^\dagger$. We will apply Lemma 3.1 to show that the second term is also negative.

Lemma 3.1. *Assume that $x_1,...,x_n$ are n positive numbers. Then, their arithmetic mean is greater than or equal to their geometric mean. In particular,*

$$\frac{x_1+x_2+...+x_n}{n} \geqslant \sqrt[n]{x_1...x_n}.$$

Now, let

$$x_1 = \frac{s^\dagger}{s}, x_2 = \frac{e^\dagger si}{es^\dagger i^\dagger}, x_3 = \frac{i^\dagger e}{ie^\dagger}.$$

Notice that $x_1x_2x_3 = 1$. According Lemma 3.1, the arithmetic mean x is larger than the geometric mean x. Therefore,

$$\frac{s^\dagger}{s} + \frac{e^\dagger si}{es^\dagger i^\dagger} + \frac{i^\dagger e}{ie^\dagger} \geqslant 3.$$

Hence, the second term is negative if $\mathscr{R}_0 > 1$. All the parameters are positive, such that $V'(s,e,i) < 0$ if $\mathscr{R}_0 > 1$ and $(s,e,i) \neq (s^\dagger, e^\dagger, i^\dagger)$. Since $V(s,e,i)$ is a function that is positive definite, radially unbounded, and $V'(s,e,i) < 0$, we can conclude that EE of model (4) is globally asymptotically stable when $\mathscr{R}_0 > 1$. □

4. Optimal Control Problem

4.1. Characterization of the optimal control problem. This section is interested at investigating optimal control measures for mitigating the transmission of TB. Let the control $u(t)$ represents monitored treatment given to people with active TB. Hence, the proportion of recovery individual from active TB class is given by $\gamma_1 u(t)i + \gamma_0(1-u(t))i$ where recovery rate γ_1 will be larger than active TB who get unmonitored treatment (γ_0). Hence, we have system (4) now read as follows:

$$\begin{aligned}
\frac{ds}{dt} &= \mu - \mu s - \beta si, \\
\frac{de}{dt} &= \beta si - \mu e - \varepsilon e, \\
\frac{di}{dt} &= \varepsilon e - \mu i - \gamma_1 u(t)i - \gamma_0(1-u(t))i, \\
\frac{dr}{dt} &= \gamma_1 u(t)i - \gamma_0(1-u(t))i - \mu r.
\end{aligned} \tag{20}$$

Our goal is to minimize the proportion of infected individuals with TB while at the same time maintaining effective control cost. Define the objective function to be minimized as

$$J = \int_0^T (\omega_1(t)e + \omega_2 i + \omega_u u^2)dt. \tag{21}$$

The weighting parameter ω_1 is the cost associated with latent TB, ω_2 is the cost associated with active TB, and ω_u is the cost of applying monitored treatment. We choose quadratic forms to measure the control cost. We seek an optimal control $\hat{u}$ such that

$$J(\hat{u}) = \min\{J(u)|u \in U\}, \tag{22}$$

where $U = \{u : a \leq u \leq b, t \in [0,T]\}$. The conditions necessary for determining the optimal controls $\hat{u}$ that satisfies will be found through Pontryagin's Minimum Principle. We need to define Hamiltonian for deriving the necessary conditions as,

$$\begin{aligned}\mathscr{H} =& f(t,x_i,u) + \sum_{k=1}^{4} \lambda_k(g_i(t,x_i,u)),\\ =&(\omega_1 e + \omega_2 i + \omega_u u^2) + \lambda_1(\mu - \mu s - \beta si) + \lambda_2(\beta si - \mu e - \varepsilon e)\\ &+ \lambda_3(\varepsilon e - \mu i - \gamma_1 ui - \gamma_0(1-u)i) + \lambda_4(\gamma_1 ui - \gamma_0(1-u)i - \mu r),\end{aligned} \tag{23}$$

for $k = 1,2,3,4$ where λ_k is the adjoint variables while x_i describe the state variables (human compartments) for $i = 1,2,3,4$. Then, taking the partial derivatives of $\mathscr{H}$ with respect to each of the state variables yields the adjoint system given below

$$\begin{aligned}\dot{\lambda_1} &= -\frac{\partial \mathscr{H}}{\partial s} = \mu\lambda_1 + \beta i\lambda_1 - \beta i\lambda_2,\\ \dot{\lambda_2} &= -\frac{\partial \mathscr{H}}{\partial e} = -\omega_1 + \mu\lambda_2 + \varepsilon\lambda_2 - \varepsilon\lambda_3,\\ \dot{\lambda_3} &= -\frac{\partial \mathscr{H}}{\partial i} = -\omega_2 + \beta s\lambda_1 - \beta s\lambda_2 + \mu\lambda_3 + \gamma_1 u\lambda_3 + \gamma_0(1-u)\lambda_3 - \gamma_1 u\lambda_4 - \gamma_0(1-u)\lambda_4,\\ \dot{\lambda_4} &= -\frac{\partial \mathscr{H}}{\partial r} = \mu\lambda_4.\end{aligned} \tag{24}$$

with transversality conditions $\lambda_k(T) = 0$, $k = 1,2,3,4$.

The optimal control u that minimizes J over U is obtained by differentiating the Hamiltonian function, evaluated at the optimal control and set the result equal to zero. Furthermore, we obtain the optimal control $\hat{u}$,

$$\hat{u} = \min\left\{u^{\max}, \max\left\{u^{\min}, \frac{(\gamma_1 - \gamma_0)(\lambda_3 - \lambda_4)i}{2\omega_u}\right\}\right\}. \tag{25}$$

4.2. The effective reproduction number $\mathscr{R}_t$. In Section 3, we calculate the basic reproduction number of system (4), and give in the form of:

$$\mathscr{R}_0 = \frac{\varepsilon\beta}{(\mu+\varepsilon)(\mu+\gamma_1 u+\gamma_0(1-u))}.$$

When $u = u(t)$, then we can not use the term of basic reproduction number $\mathscr{R}_0$ to justify the endemic level of our model. Hence, in this section we will use the effective reproduction number of our system (20) to justify the TB will extinct or exist when $u = u(t)$ implemented. Let us define the Transition (V) and Transmission (F)matrix of system (20) as:

$$V = \begin{bmatrix} -\mu-\varepsilon & 0 \\ \varepsilon & -\mu-\gamma_1 u-\gamma_0(1-u) \end{bmatrix}, \; F = \begin{bmatrix} 0 & \beta s(t) \\ 0 & 0 \end{bmatrix}.$$

Hence, the effective reproduction number [24] is given by

$$\mathscr{R}_t = \frac{\beta\varepsilon s(t)}{(\mu+\varepsilon)(\mu+\gamma_1 u(t)+\gamma_0(1-u(t)))}. \tag{26}$$

From above expression, we have that

$$\mathscr{R}_t = \mathscr{R}_0(u(t)) \times s(t). \tag{27}$$

4.3. Numerical experiments on optimal control problem. To run the simulation in this section, we use the following parameter values:

$$\beta = 0.2568, \mu = \frac{1}{73\times 12}0, \varepsilon = 0.148, \gamma_0 = 0.104, \gamma_1 = 0.416.$$

With this set of parameter values, we have the basic reproduction number $\mathscr{R}_0 = 2.423 > 1$, which means that TB will always spread among population and tends to the endemic equilibrium if the intervention do not taken place.

4.3.1. ***Effect of initial condition*** $(s(0), e(0), i(0))$**.** In this scenario, we simulate our optimal control simulation for two different initial condition. The first initial condition represent a condition where TB is just start to spread. We called this initial condition as endemic prevention scenario, and the initial condition is given by:

$$s(0) = 0.99, e(0) = 0.005, i(0) = 0.005.$$

The second initial condition represent the condition where TB is already widely spread. We called this initial condition as endemic control scenario, and the initial condition is given by:

$$s(0) = 0.7, e(0) = 0.15, i(0) = 0.15.$$

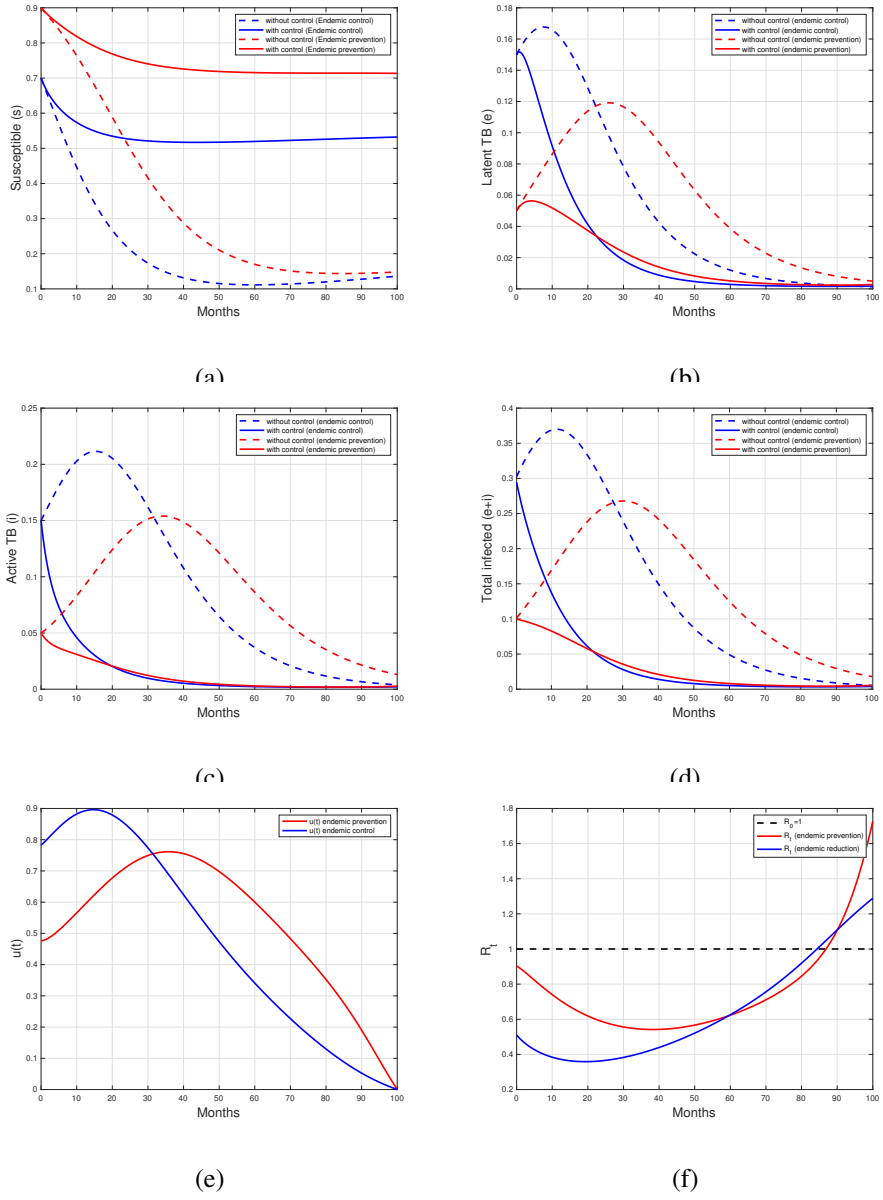

FIGURE 2. Optimal control results for endemic prevention scenario (red curve) and endemic control scenario (blue curve). Panel (a) to (f) represent the dynamic of s, e, i, $e+i$, u, and $\mathscr{R}_t$, respectively. Dashed and solid curve represent without and with control implementation, respectively.

The results are given in Figure 2 from panel (a) to (f). Red curve represent the dynamic of compartment, control, and $\mathscr{R}_t$ for endemic prevention scenario, while blue curve for endemic control scenario. From panel (a), we can see that implementation of treatment success to maintain the proportion of susceptible human still in a high number. On the other hand, from panel (b) to (d) we can see that the number of infected individuals success to be reduced when treatment control is given. We can see from panel (e) that a higher intensity of control needed for endemic control scenario at the early time of simulation. On the other hand, the dynamic of control for endemic prevention scenario is slowly increase compared to endemic control scenario. With this implementation of control, the effective reproduction number can be reduced to be smaller than one in both scenario, but slowly increase when the control intervention start to decreases. Both scenario gives $\mathscr{R}_t$ at final time of simulation to be larger than one, which indicates that endemic of TB may still occur when intervention of treatment stopped. From the calculation of cost function J in (21), we find that cost for endemic control scenario is 0.072, which is larger than endemic prevention scenario, i.e. 0.061.

4.3.2. ***Effect of initial reproduction number*** $(\mathscr{R}_0(t=0,u=0))$**.** The next simulation conducted to see the impact of initial $\mathscr{R}_0$ at $t=0$ before intervention of treatment is given. To run the simulation, we use two different set of parameter values. The first is

$$\beta = 0.2568, \mu = \frac{1}{73\times 12}0, \varepsilon = 0.148, \gamma_0 = 0.104, \gamma_1 = 0.416,$$

which gives us $\mathscr{R}_0 = 2.423$. We called this scenario as *high risk* scenario. The second set of parameter values is

$$\beta = 0.1284, \mu = \frac{1}{73\times 12}0, \varepsilon = 0.148, \gamma_0 = 0.104, \gamma_1 = 0.416,$$

which gives $\mathscr{R}_0 = 1.211$, 50% smaller than *high risk* scenario. We called this scenario as *low risk* scenario. The results are given in Figure 3.

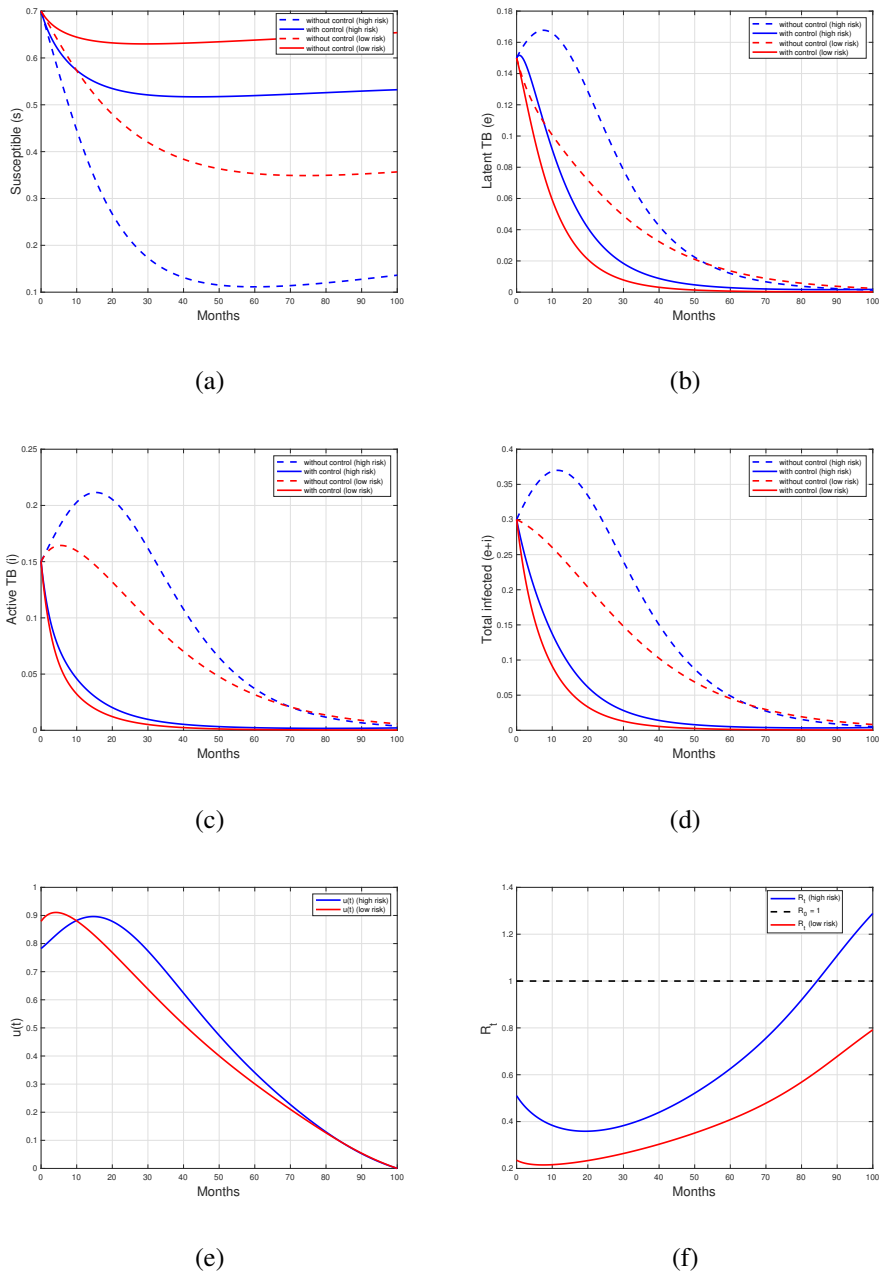

FIGURE 3. Optimal control results for low risk scenario (red curve) and high risk scenario (blue curve). Panel (a) to (f) represent the dynamic of s, e, i, $e+i$, u, and $\mathscr{R}_t$, respectively. Dashed and solid curve represent without and with control implementation, respectively.

From panel (a) in Figure 3, we can see clearly that the susceptible compartment decreases more for a *high risk* scenario compared to *low risk* scenario. Conversely, infected individuals increases more significantly for a *high risk* scenario (see panel (b) to (d)). As a results, intensity of treatment for a *high risk* scenario should be given higher in most of the time compared to the *low risk* scenario (see panel (e)). With this implementation of control, we can see that the $\mathscr{R}_t$ for *low risk* scenario is always smaller than one which indicates a bigger chance for TB eradication. On the other hand, $\mathscr{R}_t$ for *high risk* scenario becomes larger than one when the time approach the final time of simulation. As predicted, the cost for intervention for *high risk* scenario is higher than the *low risk* scenario, where $J(\textit{high risk})$=0.072, while $J(\textit{low risk})$=0.054.

4.3.3. ***Effect of control weight parameters*** (ω_u)**.** The third simulation conducted to see the impact of unit cost for control (ω_i). For this purposes, we use parameter values as follows:

$$\beta = 0.2568, \mu = \frac{1}{73 \times 12}0, \varepsilon = 0.148, \gamma_0 = 0.104, \gamma_1 = 0.416,$$

with initial condition

$$s(0) = 0.7, e(0) = 0.15, i(0) = 0.15,$$

except ω_u which varied. We choose $\omega_u = 0.1$ to represent cheap control and $\omega_u = 0.5$ to represent expensive control. The results are given in Figure 4.

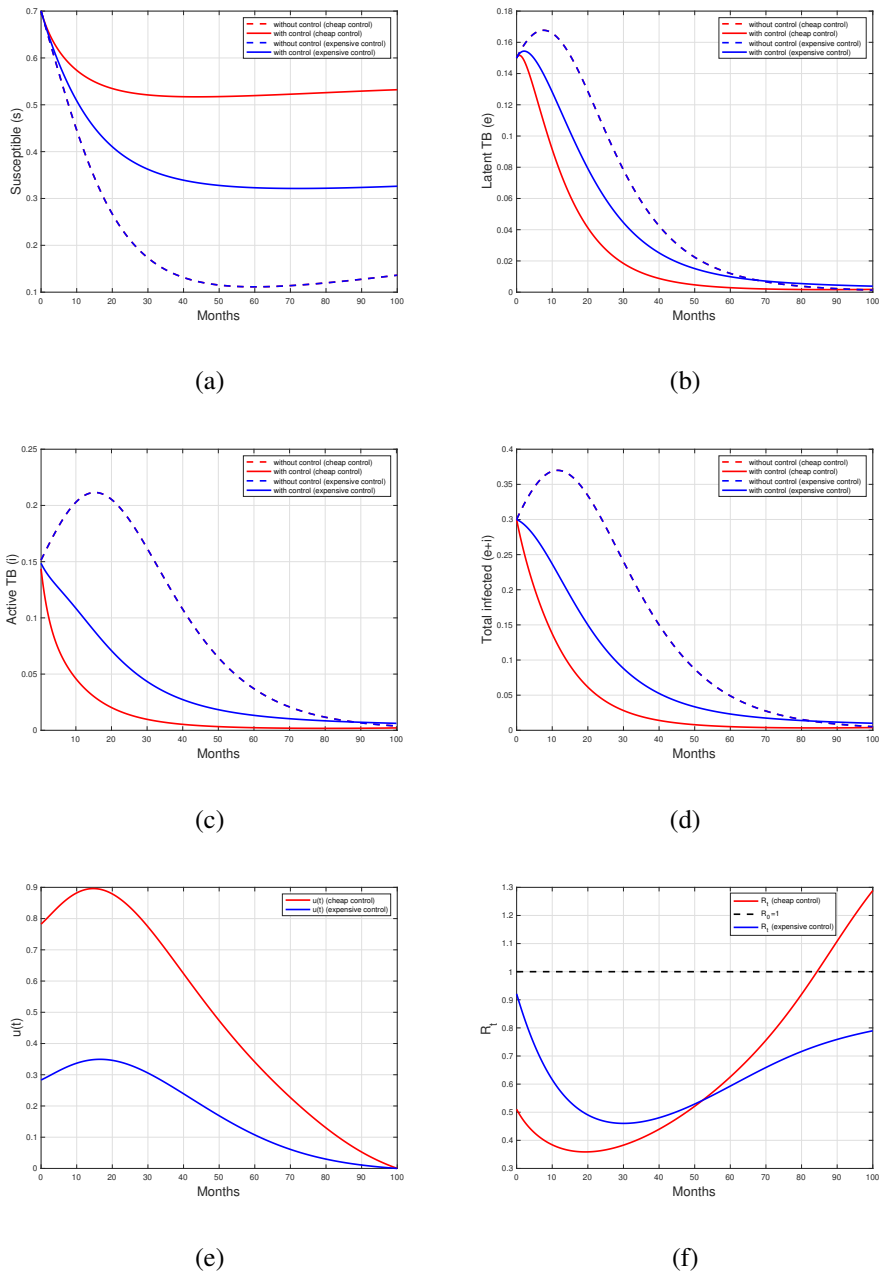

FIGURE 4. Optimal control results for cheap control scenario (red curve) and expensive control scenario (blue curve). Panel (a) to (f) represent the dynamic of s, e, i, $e+i$, u, and $\mathscr{R}_t$, respectively. Dashed and solid curve represent without and with control implementation, respectively.

We can see that the dashed blue and red which represent the dynamic before control is given are the same in panel (a) to (d). On the other hand, we can see in panel (e) that the dynamic of control for a cheap control (red) given in a higher intensity in all time of simulation compared to the expensive control scenario (blue curve). As a results, the cost for intervention for expensive control is 0.101, which is higher compared to the cheap control scenario which only 0.072, or 28.7% cheaper than the expensive control. Similar with previous result, we can see that the number of infected individual can be reduced significantly, where cheap control scenario gives a better result. The dynamic of effective reproduction number is given in panel (f), where we can see that the $\mathscr{R}_t$ for cheap control is larger than expensive control scenario. The reason is due to a higher number of susceptible individual for cheap control scenario at time $t = 100$ compared to expensive control scenario.

4.3.4. ***Effect of treatment quality*** (γ_1). In the last simulation, we conduct a numerical experiment to understand the impact of the treatment quality, which represent by γ_1. Initial condition that we used are as follows:

$$s(0) = 0.7, e(0) = 0.15, i(0) = 0.15,$$

with parameter values are:

$$\beta = 0.2568, \mu = \frac{1}{73 \times 12}0, \varepsilon = 0.148, \gamma_0 = 0.104,$$

where $\gamma_1 = 0.416$ represent the medium quality of treatment, and $\gamma_1 = 0.832$ to represent a good treatment quality. The results are given in Figure 5.

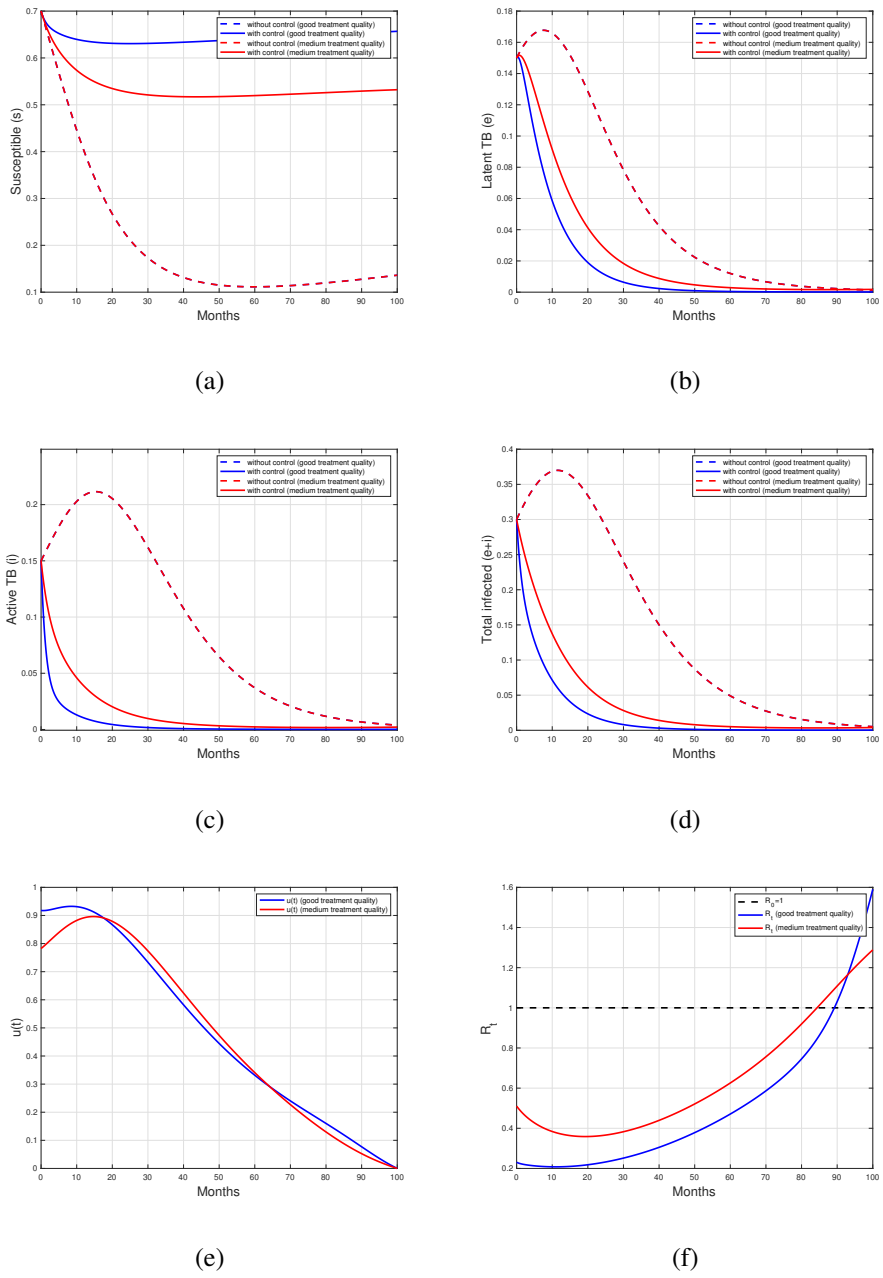

FIGURE 5. Optimal control results for good treatment quality (red curve) and medium treatment quality scenario (blue curve). Panel (a) to (f) represent the dynamic of s, e, i, $e+i$, u, and $\mathscr{R}_t$, respectively. Dashed and solid curve represent without and with control implementation, respectively.

From Figure 5, we can see that intervention of treatment with a better quality treatment gives a better result in reducing number of infected individuals (see panel (b)-(d)). The intensity of treatment that been implemented is more intense for a medium treatment quality scenario as a feedback lower recovery rate γ_1 (see blue curve in panel (e)). With this intervention, we can see clearly that $\mathscr{R}_t$ for a good treatment quality scenario is almost always smaller than the medium treatment quality scenario. However, when the time close to the final time of simulation, $\mathscr{R}_t$ increasing more rapid for the good treatment quality scenario compared to the medium treatment quality scenario. With this scenario, we find that the cost function for medium treatment quality is 0.072, while for the good treatment quality scenario is 0.0540.

5. Discussion and Conclusion

The quality of tuberculosis (TB) treatment has greatly improved recently as a result of developments in healthcare practices and medical research. To guarantee total eradication of the germs, a series of antibiotics is administered over a certain period of time as part of the usual treatment for tuberculosis. More patient-centric methods, more accessible medication, and shorter, more effective drug regimens have been the main advances in tuberculosis treatment.

Here we have modified a mathematical model for Tuberculosis (TB) employing a modified SEIR framework by authors in [13]. This model intricately incorporates the proportion of infected individuals who receive treatment, recognizing the crucial role of timely intervention in controlling the spread of TB. Furthermore, the treatment fraction is represented as a time-dependent variable within the model. This technique enables for the application of control optimum theory to discover and implement solutions that minimize number of infected individuals with optimal budget, contributing to more effective and targeted efforts toward TB eradication.

Form analytical results, when the control reproduction number is less than one, the tuberculosis (TB) free equilibrium shows both local and global asymptotic stability. On the other hand, the equilibrium becomes unstable if the reproduction number is greater than one, highlighting the crucial threshold for tuberculosis control. Additionally, it is demonstrated that the unique endemic equilibrium is unstable when the control reproduction number is below one and locally and globally asymptotically stable when the control reproduction number is larger than one.

The control optimal problem has been characterized by the application of the Pontryagin Maximum Principle [25]. The forward-backward sweep approach has been applied to successfully address the optimal control problem [26, 27, 28]. Numerical experiment conducted to give a better understanding of the optimal dynamic of tuberculosis treatment under some specific scenario. Several important finding found from our numerical experiments. The potential of treatment as a pivotal tool in controlling the widespread dissemination of Tuberculosis (TB) is shown. Notably, the effectiveness of TB control measures is contingent on the timing and intensity of interventions. A more robust and costlier treatment approach becomes imperative when dealing with advanced stages of TB dissemination, underscoring the importance of early implementation to mitigate both the spread and economic burden. Increasing intervention intensity to the population's risk, as indicated by a higher basic reproduction number, becomes crucial. In this context, an intensified intervention is essential to reduce the effective reproduction number to below one. Moreover, the optimization of TB intervention costs is achievable through the provision of superior yet cost-effective treatment options, emphasizing the significance of enhancing both the quality and affordability of interventions in the fight against TB.

ACKNOWLEDGMENTS

The authors thanks to all reviewers for their valuable comments. This research is funded by Universitas Indonesia with PUTI Q1 Research grant scheme 2023 (ID: NKB-485/UN2.RST/HKP.05.00/2023)

CONFLICT OF INTERESTS

The author(s) declare that there is no conflict of interests.

REFERENCES

[1] D. Aldila, J.P. Chávez, K.P. Wijaya, et al. A tuberculosis epidemic model as a proxy for the assessment of the novel M72/AS01E vaccine, Commun. Nonlinear Sci. Numer. Simul. 120 (2023), 107162. https://doi.org/10.1016/j.cnsns.2023.107162.

[2] Centers for Disease Control and Prevention, Treatment for latent TB infection and TB disease, (2016). https://www.cdc.gov/tb/topic/treatment/default.htm.

[3] D. Aldila, Dynamical analysis on a malaria model with relapse preventive treatment and saturated fumigation, Comput. Math. Methods Med. 2022 (2022), 1135452. https://doi.org/10.1155/2022/1135452.

[4] B.D. Handari, R.A. Ramadhani, C.W. Chukwu, et al. An optimal control model to understand the potential impact of the new vaccine and transmission-blocking drugs for malaria: a case study in Papua and West Papua, Indonesia, Vaccines. 10 (2022), 1174. https://doi.org/10.3390/vaccines10081174.

[5] H. Tasman, D. Aldila, P.A. Dumbela, et al. Assessing the impact of relapse, reinfection and recrudescence on malaria eradication policy: a bifurcation and optimal control analysis, Trop. Med. Infect. Dis. 7 (2022), 263. https://doi.org/10.3390/tropicalmed7100263.

[6] D. Aldila, Optimal control for dengue eradication program under the media awareness effect, Int. J. Nonlinear Sci. Numer. Simul. 24 (2023), 95–122. https://doi.org/10.1515/ijnsns-2020-0142.

[7] D. Aldila, M.Z. Ndii, N. Anggriani, et al. Impact of social awareness, case detection, and hospital capacity on dengue eradication in Jakarta: A mathematical model approach, Alexandria Eng. J. 64 (2023), 691–707. https://doi.org/10.1016/j.aej.2022.11.032.

[8] D. Aldila, A. Islamilova, S.H.A. Khosnaw, et al. Forward bifurcation with hysteresis phenomena from atherosclerosis mathematical model, Commun. Biomath. Sci. 4 (2021), 125–137. https://doi.org/10.5614/cbms.2021.4.2.4.

[9] D. Aldila, M. Angelina, Optimal control problem and backward bifurcation on malaria transmission with vector bias, Heliyon. 7 (2021), e06824. https://doi.org/10.1016/j.heliyon.2021.e06824.

[10] Centers for Disease Control and Prevention, Drug-Resistant TB, (2022). https://www.cdc.gov/tb/topic/drtb/default.htm.

[11] D.K. Das, S. Khajanchi, T.K. Kar, The impact of the media awareness and optimal strategy on the prevalence of tuberculosis, Appl. Math. Comput. 366 (2020), 124732. https://doi.org/10.1016/j.amc.2019.124732.

[12] D.K. Das, S. Khajanchi, T.K. Kar, Transmission dynamics of tuberculosis with multiple re-infections, Chaos Solitons Fractals. 130 (2020), 109450. https://doi.org/10.1016/j.chaos.2019.109450.

[13] K. Das, B.S.N. Murthy, Sk.A. Samad, et al. Mathematical transmission analysis of SEIR tuberculosis disease model, Sensors Int. 2 (2021), 100120. https://doi.org/10.1016/j.sintl.2021.100120.

[14] T. Iskandar, N.A. Chaniago, S. Munzir, et al. Mathematical model of tuberculosis epidemic with recovery time delay, AIP Conf. Proc. 1913 (2017), 020021. https://doi.org/10.1063/1.5016655.

[15] O. Diekmann, J.A.P. Heesterbeek, M.G. Roberts, The construction of next-generation matrices for compartmental epidemic models, J. R. Soc. Interface. 7 (2009) 873–885. https://doi.org/10.1098/rsif.2009.0386.

[16] B.D. Handari, D. Aldila, E. Tamalia, et al. Assessing the impact of medical treatment and fumigation on the superinfection of malaria: a study of sensitivity analysis, Commun. Biomath. Sci. 6 (2023), 51–73. https://doi.org/10.5614/cbms.2023.6.1.5.

[17] I.H. Febiriana, V. Adisaputri, P.Z. Kamalia, et al. Impact of screening, treatment, and misdiagnose on lymphatic filariasis transmission: a mathematical model, Commun. Math. Biol. Neurosci. 2023 (2023), 67. https://doi.org/10.28919/cmbn/7983.

[18] D. Aldila, C. Aulia Puspadani, R. Rusin, Mathematical analysis of the impact of community ignorance on the population dynamics of dengue, Front. Appl. Math. Stat. 9 (2023), 1094971. https://doi.org/10.3389/fams.2023.1094971.

[19] D. Aldila, M. Shahzad, S.H.A. Khoshnaw, et al. Optimal control problem arising from COVID-19 transmission model with rapid-test, Results Phys. 37 (2022), 105501. https://doi.org/10.1016/j.rinp.2022.105501.

[20] D. Aldila, T. Windyhani, Backward bifurcation emerging from a mathematical model of African animal trypanosomiasis disease in white rhino populations, J. Math. Fund. Sci. 54 (2022), 151–189. https://doi.org/10.5614/j.math.fund.sci.2022.54.1.9.

[21] I.M. Wangari, L. Stone, Backward bifurcation and hysteresis in models of recurrent tuberculosis, PLoS ONE. 13 (2018), e0194256. https://doi.org/10.1371/journal.pone.0194256.

[22] WHO, What is DOTS? A guide to understanding the WHO-recommended TB control strategy known as DOTS, World Health Organization, Geneva, 1999.

[23] WHO, Global Tuberculosis report 2022, World Health Organization, Geneva, (2022). https://www.who.int/teams/global-tuberculosis-programme/tb-reports/global-tuberculosis-report-2022.

[24] S. Zhao, S.S. Musa, J.T. Hebert, et al. Modelling the effective reproduction number of vector-borne diseases: the yellow fever outbreak in Luanda, Angola 2015–2016 as an example, PeerJ. 8 (2020), e8601. https://doi.org/10.7717/peerj.8601.

[25] A. Seierstad, K. Sydsaeter, Optimal control theory with economic applications, North-Holland, Amsterdam, (1987).

[26] D. Aldila, N. Awdinda, Fatmawati, et al. Optimal control of pneumonia transmission model with seasonal factor: Learning from Jakarta incidence data, Heliyon. 9 (2023), e18096. https://doi.org/10.1016/j.heliyon.2023.e18096.

[27] E.L. Megawati, D. Aldila, A stability and optimal control analysis on a dengue transmission model with mosquito repellent, Commun. Math. Biol. Neurosci. 2023 (2023), 98. https://doi.org/10.28919/cmbn/8134.

[28] D. Aldila, N. Nuraini, E. Soewono, Optimal control problem in preventing of swine flu disease transmission, Appl. Math. Sci. 8 (2014), 3501–3512. https://doi.org/10.12988/ams.2014.44275.

[29] E.P. Hafidh, N. Aulida, B.D. Handari, et al. Optimal control problem from tuberculosis and multidrug resistant tuberculosis transmission model, AIP Conf. Proc. 2023 (2018), 020223. https://doi.org/10.1063/1.5064220.